Influence of muscle recruitment criteria on joint reaction forces during human gait

Florian Michaud[*], **Urbano Lugris**[*], **Ye Ou**[#], **Javier Cuadrado**[*], **Andres Kecskemethy**[#]

[*] Lab. of Mechanical Engineering
University of La Coruña
Escuela Politecnica Superior
Mendizabal s/n, 15403 Ferrol, Spain
florian.michaud@udc.es

[#] Institute of Mechanics and Robotics
University of Duisburg-Essen
Lotharstr. 1, 47057 Duisburg,
Germany
andres.kecskemethy@uni-due.de

ABSTRACT

This paper addresses the comparison of several muscle recruitment criteria and their effect on the calculated joint reaction forces at hip, knee and ankle level during gait. Both the kinematics and the ground reactions are experimentally obtained from a female subject and applied to a three-dimensional skeletal human model featuring 43 muscles in the right leg. An inverse dynamic analysis provides the histories of the joint drive torques. Then, static –four criteria– and physiological approaches are used to estimate the muscle forces from which the joint reaction forces are calculated and can then be compared. It is concluded that significant differences are observed in the results. Moreover, some issues which came across in the course of the investigation are pointed out and discussed.

Keywords: Biomechanics, Gait, Muscle forces, Joint reactions, Muscle recruitment criteria.

1 INTRODUCTION

Determination of muscle forces during gait (or any other exercise) is of great interest to extract the principles of the central nervous system (CNS) control [1] (assessment of pathological gait from muscular activation abnormalities, diagnosis of neuromuscular disorders), or to estimate the loads on bones and joints [2] (prevention of injuries in sports, surgical planning to reconstruct diseased joints). The invasive character of *in vivo* experimental measurements, and the uncertain relation between muscle force and EMG, makes computer modeling and simulation a useful substitutive approach [3].

The fundamental problem is that there are more muscles serving each degree of freedom of the system than those strictly necessary from the mechanical point of view, which implies that, in principle, an infinite number of recruitment patterns are acceptable. This problem is often referred to as the redundancy problem of the muscle recruitment [4] or the force-sharing problem [5]. Experimental studies [6] and EMG collections [7] suggest that a specific strategy of muscle coordination is chosen by the CNS to perform a given motor task.

A popular mathematical approach for solving the muscle recruitment problem is the optimization method, which can be associated to inverse or forward dynamics [8]. These methods minimize or maximize some criterion (objective function or cost function) which reflects the mechanism used by the CNS to recruit muscles for the movement considered. The proper cost function is not known a priori, so the adequacy of the chosen function must be validated according to the obtained results [9]. Many criteria have been proposed in the literature to predict muscle forces. However, according to Daniel [10], the choice of the optimization criterion does not influence the hip reaction force in the inverse dynamic analysis.

In this work, the gait of a female subject has been analyzed and the muscle forces of the right leg have been obtained by applying both static (four different criteria) and physiological approaches. The objective is to compare the joint reaction forces at hip, knee and ankle level and to observe whether significant discrepancies appear depending on the selected method.

The remaining of the paper is organized as follows. Section 2 presents the experiment carried out and the human model used. Section 3 addresses the application of the static optimization approach to get the muscle forces, describes the four muscle recruitment criteria that have been compared in the work, and shows the obtained joint reaction forces. Section 4 explains the physiological optimization approach and provides the corresponding joint reaction forces. Finally, the conclusions of the paper are drawn in Section 5.

2 EXPERIMENT AND MODEL

The subject selected to perform the experiment is a healthy adult female, 28 years old, mass 50 kg and height 1.67 m. She walks on a walkway featuring two embedded force plates (AMTI, AccuGait sampling at 100 Hz). The motion is captured by 12 optical infrared cameras (Natural Point, OptiTrack FLEX:V100 also sampling at 100 Hz) that compute the position of 37 optical markers.

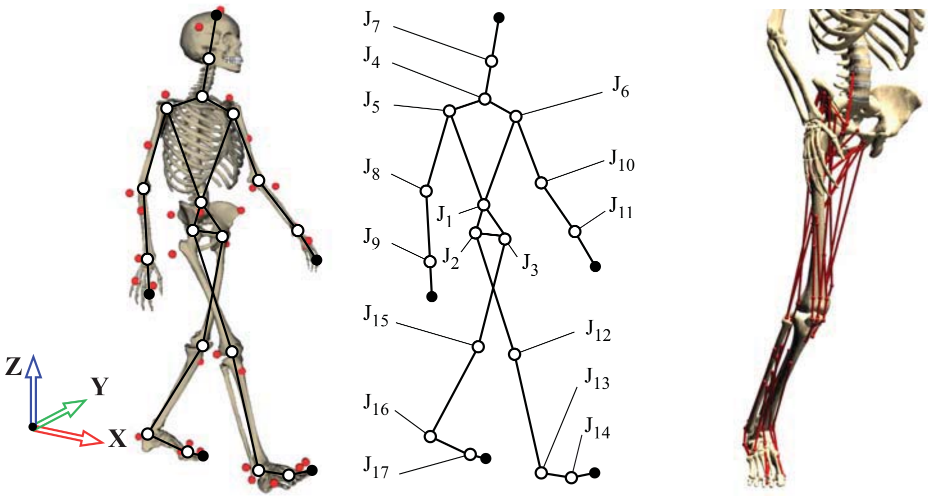

Figure 1. 3D human model and detail of muscles on the right leg.

The human body is modeled as a 3D multibody system formed by rigid bodies, as shown in Figure 1 (left and center). It consists of 18 anatomical segments: two hindfeet, two forefeet, two shanks, two thighs, pelvis, torso, neck, head, two arms, two forearms and two hands. The segments are linked by ideal spherical joints, thus defining a model with 57 degrees of freedom. The global axes are defined as follows: x-axis in the antero–posterior direction, y-axis in the medio–lateral direction, and z-axis in the vertical direction. The computational model is defined with 228 mixed (natural + angular) coordinates. The subset of natural coordinates comprises the three Cartesian coordinates of 22 points, and the three Cartesian components of 36 unit vectors, thus making a total of 174 variables. The points correspond to the positions of all the spherical joints (white dots in Figure 1, left and center), along with points of the five distal segments - head, hands and forefeet- (black dots in Figure 1, left and center). Each one of the 18 bodies is defined by its proximal and distal points, plus two orthogonal unit vectors aligned at the antero–posterior and medio–lateral directions, respectively, when the model is in a standing posture. The remaining 54 variables are the 18 sets of 3 angles that define the orientation of each body with respect to the inertial frame.

The geometric and inertial parameters of the model are obtained, for the lower limbs, by applying correlation equations from a reduced set of measurements taken on the subject, following the procedures described in [11]. For the upper part of the body, data from standard tables [8] is scaled according to the mass and height of the subject. In order to adjust the total mass of the subject, a second scaling is applied to the inertial parameters of the upper part of the body.

The kinematic information of the motion is obtained from the trajectories of the 37 markers attached to the subject's body (red dots in Figure 1, left), which are captured at 100 Hz frequency by means of the 12 infrared cameras. Position data are filtered using an algorithm based on Singular Spectrum Analysis (SSA) and the natural coordinates of the model are calculated using algebraic relations. Afterwards, a minimization procedure ensures the kinematic consistency of the natural coordinates. From that information, the histories of a set of 57 independent coordinates -as many as the system degrees of freedom- formed by the Cartesian coordinates of the position vector of the lumbar joint and the 18 x 3 angles that define the absolute orientation of each body, are kinematically obtained and approximated by using B-spline curves. Analytical differentiation yields the corresponding velocity and acceleration histories. More detail about the treatment of the captured data can be found in [12].

The matrix-R formulation [13] is applied to obtain the ground reactions and joint drive torques along the motion. Measurements from the force plates are just used to overcome the indeterminacy in the distribution of ground reactions during the double support phase. Therefore, after the analysis, a set of joint drive torques and external reactions is available which is consistent with the corresponding motion.

In the right leg of the model, 43 muscles have been considered (Figure 1, right). The properties of the muscles have been taken from OpenSim [14], which are defined for the OpenSim reference model. A scale factor is derived for each segment by comparing its dimensions with those of the reference model. This factor is applied to obtain the corrected location of insertion points in the segment. Then, lengths of muscles are calculated and compared with their counterparts in the reference model, thus yielding a scale factor for each muscle. This scale factor is applied to muscle parameters as the tendon slack length and the optimal muscle fiber length. However, no recommendation has been found in the literature on how to scale the muscle maximum isometric force, which could be expected to significantly vary among different subjects.

3 STATIC OPTIMIZATION

The first approach considered is static optimization. Since only muscles in the right leg have been modeled, joint drive torques at the right hip, knee and ankle should be reproduced by the muscle forces. The following optimization problem is stated,

$$\begin{aligned} &\min \; C \\ &\text{subject to} \quad \mathbf{J}^{\mathrm{T}}\mathbf{F} = \mathbf{Q} \\ &\qquad\qquad\quad 0 \le F_i \le F_{i,0} \quad i = 1,2,\ldots,m \end{aligned} \tag{1}$$

where C is the cost function, $\mathbf{Q}$ is the vector of joint drive torques at the right leg (where the force-sharing problem is addressed), $\mathbf{F}$ is the vector of muscle forces, $\mathbf{J}$ is the Jacobian whose transpose projects the muscle forces into the joint drive torques space, and $F_{i,0}$ is the maximum isometric force of muscle i, with m the number of muscles (in this case, 43).

Regarding the cost function C, four cases have been considered and compared, whose mathematical formulations are shown in Table 1:

I) Sum of the squares of muscle forces.

II) Sum of the squares of proportional muscle forces.

III) Sum of muscle stresses, with A_i the cross sectional area of muscle i.

IV) Largest relative muscle force.

Table 1. The four muscle recruitment criteria compared.

I	II	III	IV
$\sum_{i=1}^{m} F_i^2$	$\sum_{i=1}^{m} \left(\frac{F_i}{F_{i,0}} \right)^2$	$\sum_{i=1}^{m} \left(\frac{F_i}{A_i} \right)^2$	$\max \left\{ \frac{F_i}{F_{i,0}} \right\} \quad i = 1, 2, ..., m$

Before showing the results, there is an issue which deserves to be mentioned. Vector **Q** in (1) gathers the joint drive torques at the right hip, knee and ankle. Since there are bi-articular muscles, i.e. muscles spanning more than one joint, the optimization problem cannot be carried out on a joint-by-joint basis, but instead all the joints should be taken into account at the same time. On the other hand, it has been said when describing the human model that spherical kinematic pairs have been considered for all the joints. This means that three joint drive torques are obtained at each joint from the inverse dynamic analysis. However, not all of them are due to the actuation of muscles. For example, it is clear that the abduction/adduction torque at the knee is not provided by muscles, but rather by other joint structures as condyles and ligaments, being more a reaction moment than a drive torque. Therefore, the following joint drive torques have been selected in this work to form vector **Q**: the three torque components at the hip, the flexion/extension torque at the knee, and the plantarflexion/dorsiflexion and abduction/adduction torques at the ankle. A discussion on how the modeling of the joints and the torques considered in the optimization affect to the results can be found in [15].

Based on these assumptions, the joint reaction forces were computed at the right hip, knee and ankle for the four mentioned criteria, which are plotted in Figure 2.

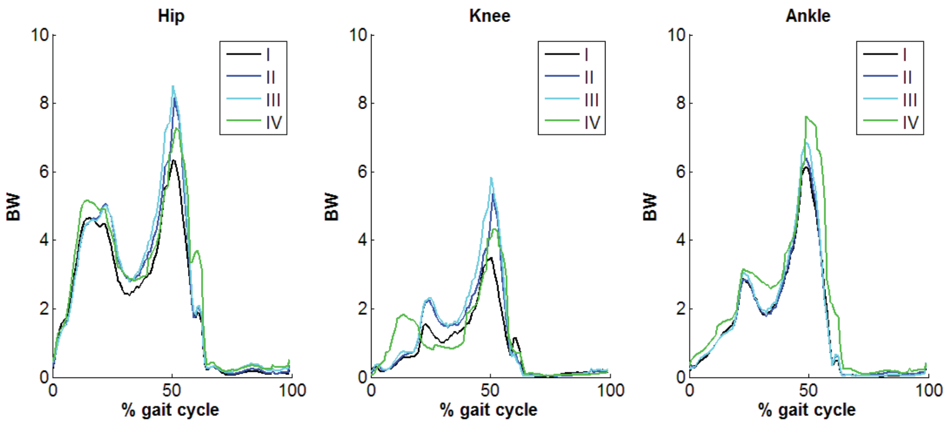

Figure 2. Joint reaction forces at hip, knee and ankle for different muscle recruitment criteria.

Conversely to what was suggested in [10], results show that different criteria lead to notably different values of the joint reaction forces. More specifically, variations of the maximum force of about 35% at the hip, 70% at the knee and 20% at the ankle can be observed in Figure 2.

4 PHYSIOLOGICAL OPTIMIZATION

In constrast to the static optimization, the so-called physiological static optimization takes muscle dynamics into account by introducing dynamic muscle force constraints [16]. This method applies static optimization techniques at each time-point but prescribes minimal and maximal constraints for the muscle forces by extrapolating the force values from the previous time-point using feasible muscle activation values. In this way, the optimization process remains efficient, but muscle dynamics are considered.

In this approach, the following optimization problem is stated,

$$\begin{aligned} &\min \sum_{i=1}^{m} \left(\frac{F_i}{F_{i,\max}} \right)^2 \\ &\text{subject to} \quad \mathbf{J}^{\mathrm{T}} \mathbf{F} = \mathbf{Q} \\ &\qquad\qquad F_{i,\min} \le F_i \le F_{i,\max} \quad i = 1, 2, ..., m \end{aligned} \tag{2}$$

where all the symbols have the same meaning as in (1), and $F_{i,\min}$, $F_{i,\max}$ are, respectively, the minimum and maximum admissible forces for muscle *i* at the corresponding time-point. In what follows, the way to determine such force limits is explained.

If the Hill's muscle model is used [17], the states of muscle *i* are denoted by the vector (index *i* is dropped for simplicity),

$$\mathbf{x} = \begin{Bmatrix} a \\ F \end{Bmatrix} \tag{3}$$

where *a* is the muscle activation and *F* is the musculotendon force. The Hill's muscle first-order differential equations are,

$$\dot{\mathbf{x}} = \begin{Bmatrix} \dot{a} \\ \dot{F} \end{Bmatrix} = \begin{Bmatrix} f_1(a,u) \\ f_2(a,F,l,v) \end{Bmatrix} = \mathbf{f}(\mathbf{x},u,l,v) \tag{4}$$

being *u* the muscle excitation, *l* the musculotendon length and *v* the musculotendon velocity.

If the states are given at a certain time *t*, the minimum and maximum state variables at time $t + \Delta t$ can be computed by setting the neural input *u* to its minimum ($u = 0$) and maximum ($u = 1$) possible values during the time interval *Δt*.

$$\begin{aligned} \mathbf{x}_{\min}(t + \Delta t) &= \mathbf{x}(t) + \int_{t}^{t+\Delta t} \mathbf{f}(\mathbf{x}, u = 0, l, v) dt \\ \mathbf{x}_{\max}(t + \Delta t) &= \mathbf{x}(t) + \int_{t}^{t+\Delta t} \mathbf{f}(\mathbf{x}, u = 1, l, v) dt \end{aligned} \tag{5}$$

The two integrations in (5) have been performed by using numerical integrator *ode23* from Matlab. Values of *l* and *v* inside the time interval *Δt* are obtained by linear interpolation of their corresponding values at times *t* and $t + \Delta t$. The solution of (5) provides the limits $F_{i,\min}$, $F_{i,\max}$ for muscle *i*. This process must be repeated for all the muscles.

It must be noted that the lowest activation at $t + \Delta t$ is not always obtained for $u = 0$. In the long term, the activation converges to the excitation value if the latter remains constant. However, for small Δt values, an excitation higher than 0 can lead to a lower activation at $t + \Delta t$. Therefore, the $F_{i,min}$ used for the optimization is not always guaranteed to be the smallest possible, although the error remains under 2.5% of the maximum activation.

Once the force limits for all the muscles have been determined, the optimization problem (2) can be solved, thus yielding the muscle forces F_i, $i = 1, 2, ..., m$ for time $t + \Delta t$. At this point, an iteration process for each muscle must be run in order to find out the (assumed constant) excitation value u_i during the time interval *Δt* that leads to the obtained muscle force F_i at time $t + \Delta t$. To that end, different values of *u* (index *i* is dropped again) are tried until the bottom part (that affecting the force; see (3)) of the following equation is satisfied,

$$\mathbf{x}(t+\Delta t)-\mathbf{x}(t)-\int_{t}^{t+\Delta t}\mathbf{f}(\mathbf{x},u,l,v)dt=0 \tag{6}$$

Function *fsolve* from Matlab has been used for the iteration process, starting with initial guess $u=1$. The bottom part of (6) is integrated for each value of u provided by *fsolve*, until the resulting muscle force falls within a certain tolerance of the force obtained in the optimization (2). The companion muscle activation can be then obtained from the upper part of (6), being the activation at time $t+\Delta t$.

So far, it has been assumed that the muscle states are known at time t in order to move to time $t+\Delta t$. Therefore, a particular procedure must be followed for the initial conditions, i.e. at time $t=0$. For that time, it is supposed that muscle velocity is zero, $v_{\mathrm{M}}=0$, for all the muscles, which implies that the force-velocity relationship of the Hill's muscle model is equal to one, $f_v(v_{\mathrm{M}}=0)=1$. To determine the initial muscle forces, the optimization problem (2) must be solved, being the force limits $F_{i,\min}$ and $F_{i,\max}$ the ones obtained by considering the minimum and maximum muscle activations, respectively, $a=0$, $a=1$. According to Figure 3, the force equilibrium demands (index i is dropped again),

$$F=F_{\mathrm{T}}=(F_{\mathrm{PE}}+F_{\mathrm{CE}})\cos\alpha \tag{7}$$

being F the musculotendon force, F_{T} the tendon force, F_{PE} the force of the parallel element, F_{CE} the force of the contractile element, and α the pennation angle.

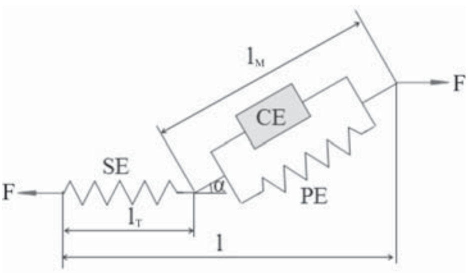

Figure 3. Hill's muscle model.

Dependencies of the previous force magnitudes are as follows: $F_{\mathrm{T}}=F_0 f_{\mathrm{T}}(l-l_{\mathrm{M}}\cos\alpha)$, $F_{\mathrm{PE}}=F_0 f_{\mathrm{PE}}(l_{\mathrm{M}})$, $F_{\mathrm{CE}}=aF_0 f_l(l_{\mathrm{M}})f_v(v_{\mathrm{M}}=0)$. Therefore, in the second equality (7), only the muscle length l_{M} is unknown, which means that it can be worked out, although in an iterative way, since the actual expressions are rather involved. Function *fsolve* from Matlab is used again for this purpose, taking the optimal muscle fiber length as initial guess.

The described problem must be solved twice for each muscle, for $a=0$ and $a=1$, respectively, thus providing, via the first equation in (7), the limits $F_{i,\min}$ and $F_{i,\max}$ required for the optimization problem (2) at the initial time, $t=0$. Once the optimization problem has been solved, the initial force of each muscle F_i is obtained, and the corresponding initial activation a_i can be derived by equaling the leftmost and rightmost equality side in (7).

A more detailed explanation of this method can be found in [18].

The joint reaction forces obtained at the right hip, knee and ankle by application of the described physiological method are plotted in Figure 4, along with the results obtained in the previous Section for the static methods, so that comparison is easily established.

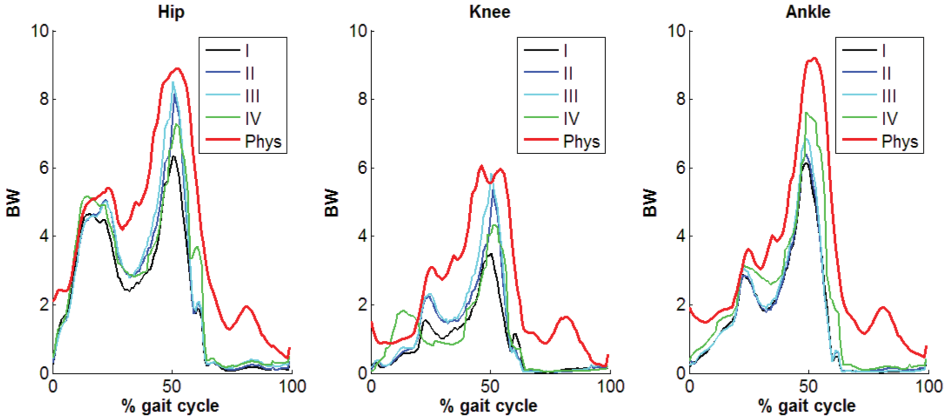

Figure 4. Joint reaction forces at hip, knee and ankle for static and physiological methods.

As it can be seen in Figure 4, the physiological method leads to even greater reaction forces that its static counterparts, thus confirming the influence of the calculation approach in the results.

5 CONCLUSIONS

The acquired gait of a female subject has been analyzed through a three-dimensional human model featuring 43 muscles in the right leg. Static optimization with four difference muscle force-sharing criteria and static-physiological optimization have been applied to estimate the histories of muscle forces, based on which, hip, knee and ankle reaction forces have been derived and compared for the five different calculation methods. Results show that the maximum joint reaction forces can significantly vary at hip, knee and ankle depending on the method selected to estimate the muscle force distribution.

It should be remarked that there are some relevant issues in the muscle force estimation process that may require further attention, like the influence of the human model degrees of freedom and the joint drive torques considered in the optimization, or the scaling of maximum isometric force of muscles.

ACKNOWLEDGMENT

The support of this work by the Spanish Ministry of Economy and Competitiveness (MINECO) under project DPI2012-38331-C03-01, confinanced by the European Union through EFRD funds, is greatly acknowledged.

REFERENCES

[1] M.R. Pierrynowski, J.B. Morrison. A physiological model for the evaluation of muscular forces in human locomotion: theoretical aspects. Mathematical Biosciences, Vol. 75, pp. 69-101, 1985.

[2] D.E. Hardt. Determining muscle forces in the leg during normal human walking – an application and evaluation of optimization methods. Transactions of the ASME, Vol. 100, pp. 72-78, 1978.

[3] A. Nagano, T. Komura, S. Fukashiro, R. Himeno. Force, work and power output of lower limb muscles during human maximal-effort counter-movement jumping. Journal of Electromyography and Kinesiology, Vol. 15, pp. 367-376, 2005.

[4] M. Damsgaard, J. Rasmussen, S.T. Christensen, E. Surma, M. de Zee. Analysis of musculoskeletal systems in the anybody modeling sustem. Simulation Modelling Practice and Theory, Vol. 14, pp. 1100-1111, 2006.

[5] J. Dul, M.A. Townsend, R. Shiavi, G.E. Johnson. Muscular synergism – I. On criteria for load sharing between synergistic muscles. Journal of Biomechanics, Vol. 17, pp. 663-673, 1984.

[6] W. Herzog, P. Binding. Cocontraction of pairs of antagonistic muscles: analytical solution for planar static nonlinear optimization approaches. Mathematical Biosciences, Vol. 118, pp. 83-95, 1993.

[7] C.A.M. Doorenbosch, G.J. van Ingen Schenau. The role of mono- and bi-articular muscles during contact control leg tasks in man. Human Movement Science, Vol. 14, pp. 279-300, 1995.

[8] J.A.C. Ambrosio, A. Kecskemethy. Multibody dynamics of biomechanical models for human motion via optimization. In J.C. Garcia Orden, J.M. Goicolea, J. Cuadrado (Eds.) Multibody Dynamics – Computational Methods and Applications, pp. 245-270, Springer, 2007.

[9] R.D. Crowninshield, R.C. Johnston, J.G. Andrews, R.A. Brand. A biomechanical investigation of the human hip. Journal of Biomechanics, Vol. 11, pp. 75-85, 1978.

[10] M. Daniel. Mathematical modelling of the hip joint loading. Bulletin of Applied Mechanics, Vol. 3, pp. 201-215, 2004.

[11] C.L. Vaughan, B.L. Davis, J.C. O'Connor. Dynamics of Human Gait (2nd ed.). Kiboho Publishers, Cape Town, 1999.

[12] U. Lugris, J. Carlin, A. Luaces, J. Cuadrado. Gait analysis system for spinal cord injured subjects assited by active orthoses and crutches, Journal of Multi-body Dynamics, Vol. 227, No. 4, pp. 363-374, 2013.

[13] J. Garcia de Jalon, E. Bayo, Kinematic and Dynamic Simulation of Multibody Systems. Springer-Verlag, New York, 1994.

[14] S.L. Delp, F.C. Anderson, A.S. Arnold, P. Loan, A. Habib, C.T. John, E. Guendelman, D.G. Thelen. OpenSim: Open-source software to create and analyze dynamic simulations of movement. IEEE Transactions on Biomedical Engineering, Vol. 54, No. 11, pp. 1940-1950, 2007.

[15] H. Mokhtarzadeh, L. Perraton, L. Fok, M.A. Muñoz, R. Clark, P. Pivonka, A.L. Bryant. A comparison of optimisation methods and knee joint degrees of freedom on muscle force predictions during single-leg hop landings. Journal of Biomechanics, Vol. 47, pp. 2863-2868, 2014.

[16] G. Pipeleers, B. Demeulenaere, I. Jonkers, P. Spaepen, G. Van der Perre, A. Spaepen, J. Swevers, J. De Schutter. Dynamic simulation of human motion: numerically efficient inclusion of muscle physiology by convex optimization. Optimization and Engineering, Vol. 9, pp. 213-238, 2008.

[17] F.E. Zajac. Muscle and tendon: properties, models, scaling, and application to biomechanics and motor control. Critical Reviews in Biomedical Engineering, Vol. 17, pp. 359-411, 1989.

[18] Y. Ou. An analysis of optimization methods for identifying muscle forces in human gait. Ph.D. dissertation. University of Duiburg-Essen. April 2012.